Journal of Hydrology: Regional Studies 19 (2018) 265–278

Contents lists available at ScienceDirect

Journal of Hydrology: Regional Studies

journal homepage: www.elsevier.com/locate/ejrh

Effects of different precipitation inputs on streamflow simulation in the Irrawaddy River Basin, Myanmar

T.A.J.G. Sirisena[a,b,*], Shreedhar Maskey[a], Roshanka Ranasinghe[a,b,c,d], Mukand S. Babel[e]

[a] Department of Water Science and Engineering, IHE Delft Institute for Water Education, Delft, The Netherlands
[b] Department of Water Engineering and Management, University of Twente, Enschede, The Netherlands
[c] Harbour, Coastal and Offshore Engineering, Deltares, Delft, The Netherlands
[d] Research School of Earth Sciences, The Australian National University, Canberra, Australia
[e] Water Engineering and Management, School of Engineering and Technology, Asian Institute of Technology, Thailand

ARTICLE INFO

Keywords:
Irrawaddy River Basin
Spatial and temporal variabilities of precipitation
Streamflow simulation

ABSTRACT

Study region: The Irrawaddy River Basin, Myanmar.
Study focus: Precipitation is the most important input variable to numerically simulate the hydrological responses of a river basin. Nowadays, a number of precipitation data products with different spatial and temporal resolutions are available. However, the accuracy of these products may vary greatly and the variations may themselves differ in different river basins. Such differences have direct implications on the use of these datasets in hydrological modelling. Here, using a hydrological model, we investigated the effects of four precipitation datasets (in-situ gauge precipitation with and without interpolation, PERSIANN-CDR, and CHIRPS) on streamflow simulations in the Irrawaddy Basin in Myanmar.
New hydrological insights for the study region: We identified considerable differences in streamflow simulation with the use of different precipitation inputs. The four datasets showed varied annual and seasonal precipitation values over the basin. Although the gauge density within the study area is very low, streamflow simulations forced with interpolated gauge data outperformed the models forced with other datasets. However, simulations forced with CHIRPS and PERSIANN-CDR also showed good results in most cases in terms of Nash Efficiency and R^2, but mostly with high biases. In calibration, the four precipitation inputs resulted in varied best-fitted parameter values and ranges. All the above observations indicate that the selection of suitable precipitation input(s) is necessary for an accurate investigation of the hydrological responses of any given basin.

1. Introduction

Precipitation is the fundamental input variable for the hydrological modelling of river basins. The accuracy of hydrological model outcomes largely depends on the quality of the precipitation data used. One major challenge in hydrological modelling is to accurately represent the spatial and temporal variations in precipitation over a river basin. Mostly, areal precipitation over a basin is estimated from in-situ gauge measurements. However, available gauged precipitation data are mostly inadequate to accurately

* Corresponding author at: Department of Water Science and Engineering, IHE Delft Institute for Water Education, PO Box 3015, 2601 DA, Delft, The Netherlands.
E-mail address: j.sirisena@un-ihe.org (T.A.J.G. Sirisena).

https://doi.org/10.1016/j.ejrh.2018.10.005
Received 16 April 2018; Received in revised form 12 October 2018; Accepted 16 October 2018
Available online 27 October 2018

represent the heterogeneity of precipitation in many river basins (Miao et al., 2015). Nowadays, radar and satellite-based remotely sensed precipitation data are being widely used as alternative sources of precipitation inputs for hydrological simulations. There are a number of precipitation products available, which vary in spatial coverage (i.e global and regional) and temporal scales (hourly, daily, and monthly). These gridded precipitation data are available for various spatial resolutions, varying from $0.05^{\circ} \times 0.05^{\circ}$ to $1^{\circ} \times 1^{\circ}$. Sources of these data include interpolated from in-situ measurements (APHRODITE, CPC Unified), reanalysis products (ERA-Interim, NCEP-CFSR, JRA-55), and remote sensing based products (CHIRPS, PERSIANN, CMORPH, GridSat, TRMM, GSMap V5/6, and SM2RAIN-ASCAT).

Many studies have investigated the impacts of different precipitation inputs on hydrological modelling (Andreassian et al., 2001; Bárdossy and Das, 2006; Lopez et al., 2015; Masih et al., 2011; Miao et al., 2015; Moon et al., 2004; Moulin et al., 2008; Price et al., 2014; Segond et al., 2007; Thiemig et al., 2013; Tuo et al., 2016; Zhu et al., 2017). For instance, Beck et al. (2017) evaluated 22 precipitation products globally, of which 13 were evaluated by comparing them to daily in-situ gauge data, and the rest were evaluated in terms of streamflow simulation using the HBV model (the Hydrologiska Byråns Vattenbalansavdelning model) (Seibert and Vis, 2012). Their results have demonstrated significant biases among the precipitation products tested. Among the non-gauge corrected precipitation datasets: CHIRP V2.0, and MSWEP-ng V1.2 and V2.0 produced the most accurate long-term mean due to the high resolution climatic datasets used. It was also noticed that gauge-corrected precipitation datasets (the CPC Unified and MSWEP versions) performed best in mid-latitude regions, where dense monitoring networks exist. In contrast, their worst performance was observed in arid regions due to highly localized and varied convective rainfall. Other studies have also indicated that all precipitation products are not equally good or bad for all regions. For example, satellite-based datasets are generally unable to accurately represent precipitation in high altitude regions (Beck et al., 2017). Furthermore, Massari et al., (2017)'s results show the relatively high performance of satellite rainfall products (3B42RT and CMORPH) in Northern and Southern America, Southern Europe, Southern Africa, and Southern and Eastern Asia. In the same study, ERA-Interim data was seen to perform reasonably well in the Northern Hemisphere, while SM2RAIN showed very good performance in the Southern Hemisphere. Whether a precipitation product is reliable or not depends also on the purpose of its use (Toté et al., 2015). For example, a precipitation product that adequately captures drought events may fail to simulate flood events and vice versa. In Toté et al. (2015)'s study, CHIRPS data showed the best model performance during the cyclone season, while RFE showed better performance in lower rainfall (10 days rainfall) situations than CHIRPS and TARCAT did. Shrestha et al. (2017) have concluded that CHG datasets (CHIRP and CHIRPS) can be used for precipitation-based drought monitoring in the Koshi Basin in Nepal.

The present study evaluates the impacts of four precipitation datasets on streamflow simulation at the Irrawaddy River Basin in Myanmar. For streamflow simulation, we used the most widely used hydrological model SWAT (Soil Water Assessment Tool) (Arnold et al., 1998; Neitsch et al., 2011). Out of the four precipitation datasets used, two sets are derived from the available in-situ measurements (with and without interpolation), while the other two are satellite-based products. The reason for using two datasets from the same in-situ gauge measurements is governed by the way precipitation input is handled in SWAT. In its default setting, SWAT assigns one precipitation gauging station to each sub-basin which is closest to basin's centroid, irrespective of the number of gauge stations available. This means that the same gauging stations may be assigned to more than one sub-basin while some gauging stations may not be assigned to any. As a result, the precipitation input to the model varies when the number of sub-basins varies. One way to avoid this issue is to spatially interpolate the gauge observations over the basin using a fixed grid and then to assign interpolated values to each sub-basin. The two remote sensing based products used in this study are PERSIANN-CDR (Ashouri et al., 2015) and CHIRPS (Funk et al., 2015). PERSIANN-CDR is an abbreviation for Precipitation Estimation from Remote Sensing Information using Artificial Neural Network – Climate Data Record and CHIRPS stands for Climate Hazard Group Infrared Precipitation with Station data. The main reason for choosing these two products was their successes reported in recent studies (Ashouri et al., 2016; Casse and Gosset, 2015; Ceccherini et al., 2015; Guo et al., 2015; Le and Pricope, 2017; Shrestha et al., 2017; Zhu et al., 2017). Simulations with PERSIANN-CDR datasets have shown reasonably good performance in streamflow prediction at two river basins (the Yangtze and the Upper Yellow River Basins) in the Tibetan Plateau (Liu et al., 2017). Based on different extreme precipitation indices, PERSIANN-CDR data is capable in reproducing daily precipitation extremes of similar spatial and temporal patterns to those produced by East Asia (EA) ground-based gridded daily precipitation datasets (Miao et al., 2015). The CHIRPS product has shown good agreement with ground-based rain gauge data all over Cyprus (Katsanos et al., 2016). Hassels (2015) compared several open access satellite-based precipitation products for the Nile River Basin and recommends CHIRPS as one of the best products available for hydrological studies in that region. Streamflow simulations with CHIRPS data have provided satisfactory results for Alpine catchments as well (Tuo et al., 2016).

Compared to the rest of the world, there are only a handful of studies that have been carried out to date to investigate the impacts of rainfall inputs on hydrological simulations in Southeast Asia, especially where ground observations are particularly sparse and limited. For example, Vu et al. (2012) found that APHRODITE performed better in daily streamflow simulation than TRMM, PERSIANN, GPCP, and CHCHN2 in the Dak Bla River Basin, Vietnam. Tan et al. (2017) evaluated three long-term gridded climatic products (APHRODITE, PERSIANN-CDR, and NCEP-CFSR) for streamflow simulation in two river basins: the Kelantan and Johor River Basins in Malaysia. Their study has shown that hydrological simulations driven by APHRODITE and PERSIANN-CDR tend to underestimate extreme precipitation and streamflow, while models driven by NCEP-CFSR are likely to overestimate the same hydrological variables. No such studies on the evaluation of rainfall products over the Irrawaddy Basin in Myanmar are to be found in the literature till date.

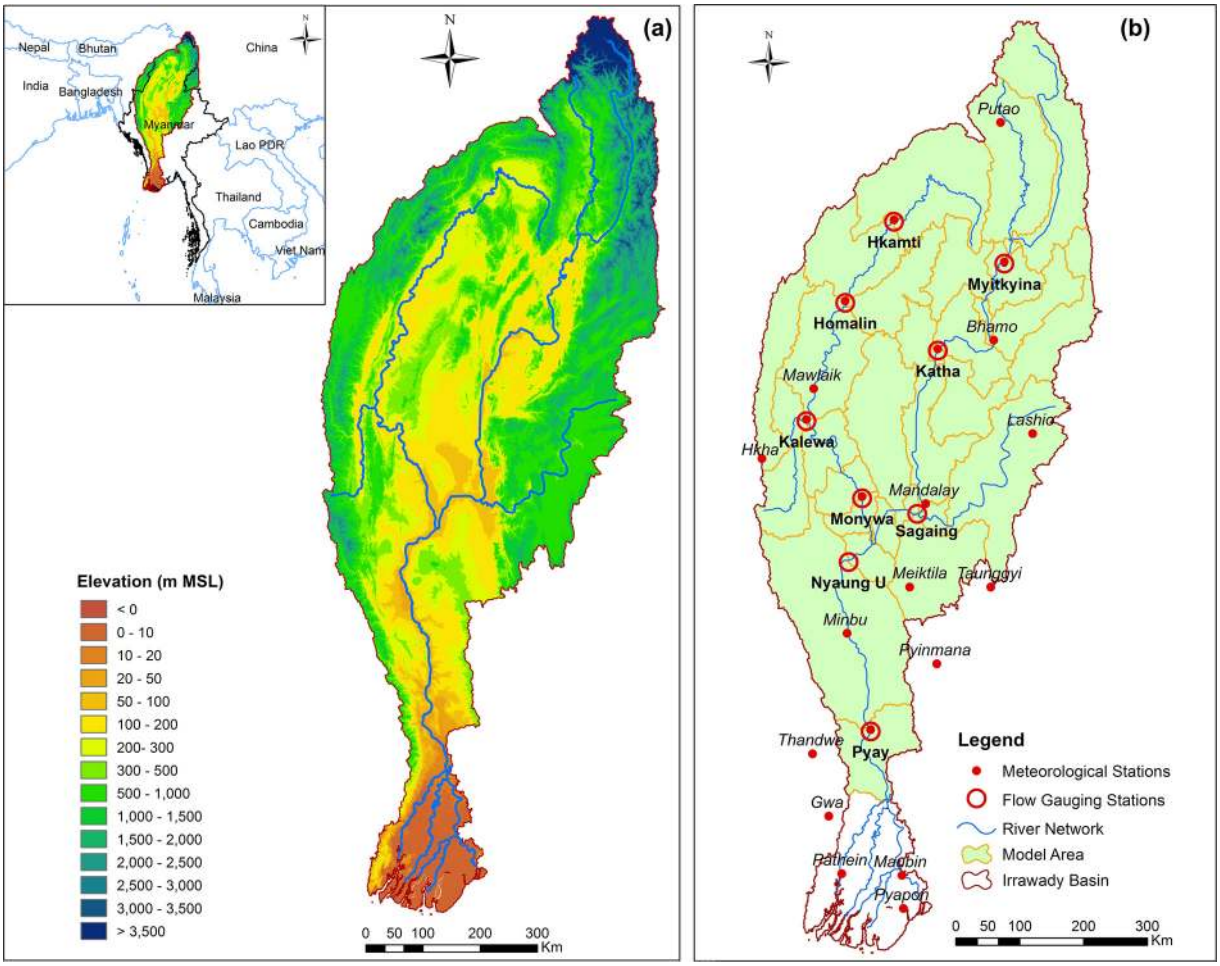

Fig. 1. Study Area (the Irrawaddy River Basin) (a) Topography of the basin (b) Delineated sub-basins and hydro-meteorological stations. Note: More details on catchment delineation are discussed in Section 2.3.

2. Materials and methods

2.1. Study area

Myanmar is the second largest country in Southeast Asia, bordered by India and Bangladesh in the west, Laos and Thailand in the east, and China in the north and northeast. In the south, it forms a coastline along the Bay of Bengal and the Andaman Sea. Irrawaddy (also known as Ayeyarwaddy) is the largest river basin in Myanmar. About 91% of the basin is located in Myanmar, while the rest is in Chinese (5%) and Indian (4%) territories. The total drainage area of the basin is approximately 410,000 km^2. The Irrawaddy River (~2100 km) is the most important commercial waterway in Myanmar. It drains into the Andaman Sea, forming one of the largest delta systems in South-East Asia (Fig. 1 (a)). The basin has diverse topographic features, ranging from high mountainous terrain in its northern part to low-lying delta systems in the south. In the middle, there are plateaus (~500 m above mean sea level (MSL)) and floodplains. Green forests and crop cultivations cover more than 60% of the basin area.

In general, Myanmar has a tropical monsoon climate. Due to the varied topography of the basin, its mean annual precipitation varies drastically from ~500 mm to ~4000 mm; the lowest and highest precipitation have been observed in the central plateaus and the northern high mountainous regions, respectively. The average annual temperature of the basin varies from 19 to 31 °C. Myanmar experiences five weather seasons: pre-monsoon (mid-April to mid-May), main monsoon (mid-May to mid-October), post- monsoon (mid-October to end-November), dry and cold (end-November to mid-March), and the hot season (mid-March to mid-April) (Qian and Lee, 2000). However, in the seasonal analysis that was performed in this study, we redistributed the seasons into three major phases: the Monsoon season (May to October), the Cold season (November to February), and the Hot season (March to April).

Table 1
Annual average statistics of streamflow data (1991–2010).

Station Name	Drainage Area (km^2)	Mean Discharge (m^3/s)	Standard Deviation (m^3/s)	Max. Discharge (m^3/s)	Min. Discharge (m^3/s)
Hkamti	27,439	2,240	662	3,563	1,199
Homalin	43,370	3,141	701	4,426	1,604
Kalewa	73,495	4,146	729	5,638	2,892
Monywa	110,926	4,569	802	6,489	3,242
Katha	84,325	5,096	583	6,133	4,015
Sagaing	124,905	7,189	1,310	9,382	5,236
Nyaung U	314,920	11,179	1,376	13,888	8,595
Pyay	359,662	12,054	1,605	14,405	9,206

2.2. Data

For catchment delineation, a 90 m × 90 m resolution Digital Elevation Model (DEM) was obtained from the Shuttle Radar Topography Mission digital topographic data (SRTM, Jarvis et al., 2008). In the SWAT model's configuration, land cover, soil, and slope data are required to define Hydrological Response Units (HRUs). HRUs are the primary computational units of the model. Land cover information at 300 m × 300 m resolution for the year 2009 was obtained from the European Space Agency, which indicated that forests (36%), different croplands (31%), and shrublands (29%) the predominant in the study area. A soil map at 7 km × 7 km resolution was obtained from Food and Agriculture Organization (FAO, 2003), in which Acrisols, Cambisols and Gleysols are the dominant types in the study basin. The slope is derived from DEM in HRU definition tool. Topographic slope classification followed the FAO (2003) slope class definitions: undulating land (0–8% slope), hilly areas (8–30% slope), and mountainous areas (> 30% slope).

Here, we used observed daily temperature (minimum and maximum) data at the weather stations for the period of 2001 to 2010 shown in the Fig. 1 (b). Furthermore, temperature data from 1990 to 2000 used in previous studies was also utilized in this study. Monthly wind speed, and relative humidity data of 5 stations (Hkamti, Homalin, Mawlaik, Kalewa and Monywa) were also used in the simulations. Observed daily streamflow data are available for 9 locations (Fig. 1 (b)) from 1991 to 2010. Based on the data availability, 8 locations (described in Table 1) were selected for this study.

Spatially varied four precipitation datasets were used (Table 2); Gauge precipitation data, Interpolated Gauge data and two satellite-based and station corrected precipitation products; PERSIANN – CDR and CHIRPS. Daily observed precipitation data of the weather stations (Fig. 1 (b)) was used for the period of 2001 to 2010. Furthermore, precipitation data from 1990 to 2000 used in previous studies were also utilized in the present study due to limited time period available for model calibration and validation. Missing data in this dataset has been filled with the Asian Precipitation Highly Resolved Observational Data Integration Towards Evaluation of Water Resources (APHRODITE) data (Yatagai et al., 2012). In this study, we used the Inverse Distance Elevation Weighted (IDEW) method to interpolate daily precipitation data from 19 gauges over a 25.5 km × 25.5 km grid. Among the various interpolation methods discussed in literature, IDEW method considers the combined effects of distance and elevation on the spatial variability of precipitation (Masih et al., 2011). This interpolation and aggregation over sub-basins were carried out using the tool Hykit, which was developed for grid-based interpolation of hydrological variables (Maskey, 2013). The corresponding parameter values were defined using the Jackknife cross validation approach (Quenouille, 1956). In this method, the data from all stations excluding the current validation station were used for interpolation. Then, the interpolated precipitation at current station is compared with corresponding grid cell. The resulting interpolated precipitation values of grid cells were then averaged over the sub-basins.

2.3. Model setup and calibration

In the catchment delineation, a drainage area threshold of 750 km^2 was used as the stream definition. Based upon the threshold and manually introduced outlet locations, total study area (371,558 km^2) was delineated into 32 sub-basins (Fig. 1 (b)). To differentiate HRUs, a threshold value of 5% was used for each land use, soil and slope data. Larger thresholds were found to eliminate any

Table 2
Overview of precipitation datasets used in this study.

Data set	Data source	Spatial Resolution	Spatial Coverage	Temporal resolution	Temporal coverage
GP	G	–	19 stations in the basin	Daily	1990–2010[a]
IGP	G	0.25°		Daily	
PERSIANN-CDR	G,S	0.25°	60°S–60°N	Daily	1983 NRT
CHIRPS	G,S	0.05°	50°N–50°S	Daily	1981 NRT

Note: G – Gauge, S – Satellite, NRT – Available until present day with several days of delay. Hereafter, Gauge precipitation data is referred as GP, interpolated gauge data as IGP, PERSIANN-CDR and CHIRPS remain the same.

[a] This period represents only the temporal coverage of observed data used in this study.

Table 3
Hydrological model parameters used in the model calibration.

Parameter	Description	Scale	Default	Initial Range
a_CN2.mgt	SCS curve number, AMC (II)	HRU	HRU Specific	−8–10
v_GWQMN.gw	Threshold groundwater depth for return flow to occur (mm)	Basin	1000	0–1000
v_GW_DELAY.gw	Groundwater delay time (days)	Basin	31	0–150
v_ALPHA_BF.gw	Base flow Alpha Factor (days)	Basin	0.048	0–1
v_CANMX.hru	Maximum canopy storage (mm)	Basin	0	0–1
v_CH_N2.rte	Manning's coefficient for main channel	Basin	0.014	0.02–0.2
v_CH_K2.rte	Hydraulic conductivity of main channel (mm/h)	Basin	0	0–100
r_SOL_AWC().sol	Available water capacity of a soul layer (mm H_2O/mm Soil)	HRU	Soil specific	−0.5–0.5
v_ESCO.hru	Soil evaporation compensation factor	HRU	0.95	0–1
v_SURLAG.hru	Surface runoff lag coefficient	HRU	2	0–10
v_EPCO.hru	Plant uptake compensation factor	HRU	1	0–1
r_OV_N.hru	Manning's coefficient for overland flow	HRU	HRU Specific	0–0.5
v_GW_REVAP.gw	Groundwater "revap" coefficient	Basin	0.02	0.02–0.2
v_REVAPMN.gw	Threshold water depth in shallow aquifer for "revap" or percolation to occur (mm)	Basin	750	0–1000

Note: a, v and r denote 'value added', 'a replacement' and 'relative change' to existing initial parameter values.

smaller definable areas of land use, soil and slope categories. On the other hand, finer thresholds would require more computing resources (Her et al., 2015). Based on the defined thresholds, 747 HRUs were created covering the entire study area.

Among the methods available in SWAT, Soil Conservation Services-Curve Number (SCS-CN) method was used to simulate surface runoff, and the variable storage method was adopted for routing the flow through channel networks. Potential evapotranspiration (PET) was calculated using the Hargreaves method (Neitsch et al., 2011), which requires less input parameters compared to other available methods in SWAT model.

The SWAT model was calibrated using monthly simulated streamflow at 8 locations (Fig. 1 (b), and Table 1). Model calibration and validation was carried out for the 1991–2000 and 2002–2010 time periods, respectively. The first year of simulations (1990 and 2001) were used as warm-up period to initialize the model state variables such as soil moisture and groundwater. Sequential Uncertainty Fitting algorithm version 2 (SUFI-2) (Abbaspour et al., 2007) in SWAT- Calibration and Uncertainty Programme (SWAT-CUP) (Abbaspour, 2015) was used for automatic model calibration and validation. A number of successful applications of SUFI-2 can be found in literature (ex. Abbaspour et al. (2015, 2007, 2004), Masih et al. (2011) and Shrestha et al. (2013)). Model parameters and their initial ranges for calibration were selected following the suggestions made in the aforementioned studies (Table 3). Modified Nash-Sutcliffe Efficiency (MNSE) (Abbaspour, 2015) was used as the objective function to optimize the model calibration, which has proven better performance than NSE as the objective function particularly in low flow (Legates and McCabe, 1999; Pushpalatha et al., 2012). Model was calibrated using different numbers of iterations, each with 500 simulations. After each iteration, the calibration program suggests a new set of parameter ranges for the next iteration. However, final parameter ranges for the subsequent iteration were obtained by considering their physically realistic upper and lower limits. The iteration process was terminated, when no significant improvement in the model performance was observed between two successive iterations. Once a gauging station is calibrated, relevant parameters were fixed for all the sub-basins drain to that gauging station. Then the initial parameter ranges were set for the subsequent downstream gauging station for calibration. This procedure was repeated for each of the discharge locations starting from upstream and continued to downstream of the basin. The calibrated parameter ranges were used for the validation period with 500 simulations. This method was repeated for the model simulations with the four different precipitation datasets.

Although, MNSE was used as the objective function, model performances were assessed using most commonly used three indicators; NSE, coefficient of determination (R^2) and Percentage Bias (PBIAS). We have adopted criteria recommended by Moriasi et al. (2007) to classify the model performance as very good ($0.75 < NSE \leq 1$), good ($0.65 < NSE \leq n\,0.75$), satisfactory ($0.5 < NSE \leq 0.65$) and unsatisfactory ($NSE \leq 0.5$).

2.4. Uncertainty assessment

Uncertainties in streamflow prediction can be introduced from different sources such as input data, the model parameters, and the model structure (Abbaspour, 2015; Pechlivanidis et al., 2011). SUFI-2 is a commonly used tool for auto-calibration and uncertainty assessment for the SWAT model. In SUFI-2, the total uncertainty in the model result (streamflow) is estimated in terms of parameter uncertainty based on a deterministic set of input (forcing) data (e.g. precipitation and temperature). It uses two measures, called r-factor and P-factor, to express the total uncertainty. The r-factor is defined as the ratio of the average width of the 95 percent prediction uncertainty (95PPU) band to the standard deviation of observed data. The 95PPU band is derived from the model outputs based on randomly generated model parameter sets. The P-factor, which ranges from 0 to 1, represents the fraction of observation data points contained within 95PPU. Ideally, the P-factor should be 0.95 to represent 95% of the total uncertainty. However, it is rarely the case in practice; the P-factor is usually less than 0.95, meaning that the parameter uncertainty with the estimated r-factor is unable to fully represent the total uncertainty. Given the precipitation as primary forcing data in the SWAT model as in any hydrological model, it may represent a major source of uncertainty. However, we did not have quantitative information to present uncertainty in each of the four precipitation products used in this study. Moreover, our approach here was to evaluate the ability of

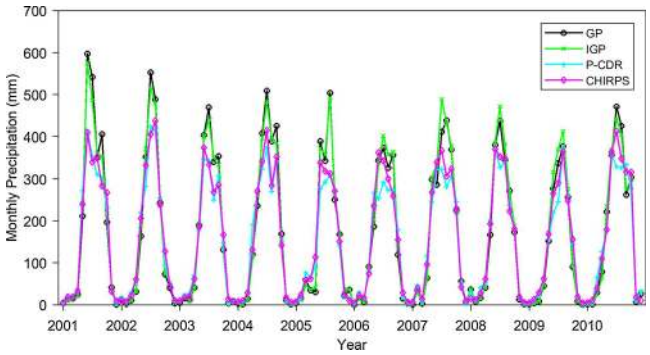

Fig. 2. Monthly precipitation of four precipitation datasets over the study area.

these products to simulate streamflows using a hydrological model. The ability of each product was assessed in terms of the model performance indicators such as NSE, R^2, and PBIAS, and the total uncertainty measures r-factor and P-factor, as mentioned above.

3. Results and discussion

3.1. Comparison of precipitation datasets

Monthly precipitation patterns of the four datasets (Fig. 2) show that PERSIANN-CDR and IGP data yield the lowest and highest precipitation, respectively, throughout the 10 year period (2001 to 2010) considered. Monthly precipitation of PERSIANN-CDR and CHIRPS was lower than the IGP in each year, particularly during the months from June to August. The difference between GP and IGP is marginal (about 32 mm/year), which is mostly attributed to the fact that the two datasets are generated from the same observed rain gauge data. The total precipitation of CHIRPS was relatively less than IGP data (170 mm/year), whereas PERSIANN-CDR showed the highest difference in total precipitation (235 mm/year).

Variations in average annual precipitations over the sub-basins are presented in Fig. 3. Precipitation based on IGP data varied from 1000 mm in the middle to 3400 mm in the northern part of the basin with a standard deviation of 622 mm. The highest variation was observed with GP data (750 mm to 4400 mm), with a standard deviation of 994 mm. PERSIANN-CDR precipitation varied from 1000 mm to 2700 mm (with a standard deviation of 357 mm), and CHIRPS precipitation varied between 800 mm to 3000 mm (with a standard deviation of 560 mm). PERSIANN-CDR and CHIRPS differed notably from IGP in the most upstream sub-basin areas, but those differences become smaller towards the most downstream areas.

Fig. 4 shows the variations among the four datasets across the three main seasons (hot, monsoon, and cold) considered. Spatial

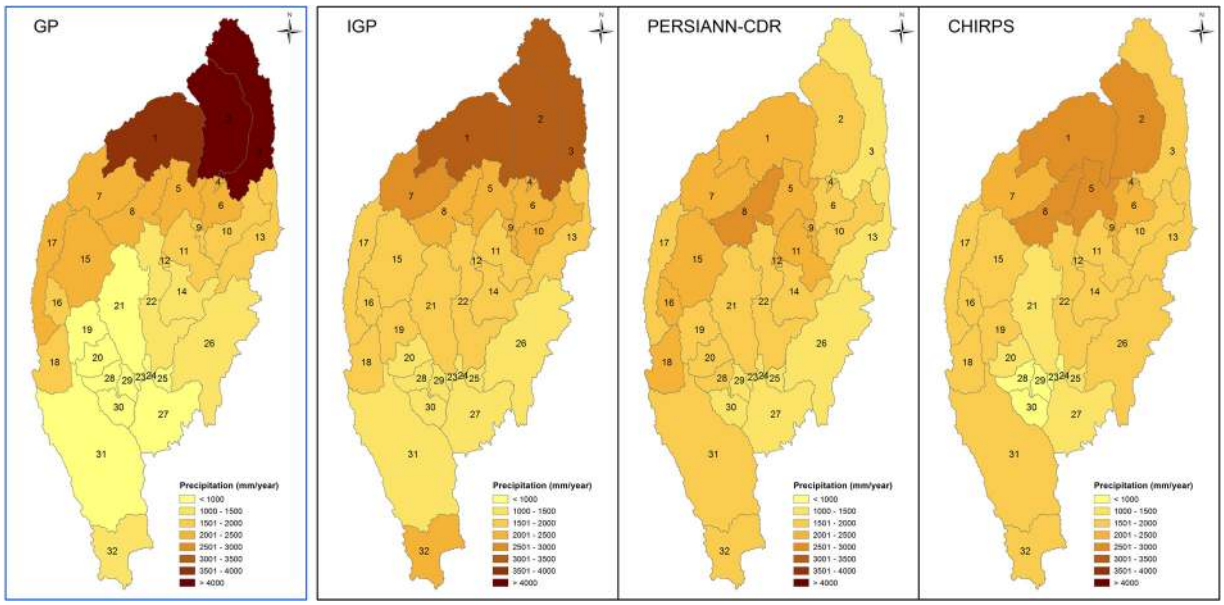

Fig. 3. Spatial distribution of average annual precipitation values for the four precipitation datasets considered (2001–2010). From left to right: GP (Gauge precipitation), IGP (Interpolated gauge precipitation), PERSIANN-CDR, and CHIRPS data.

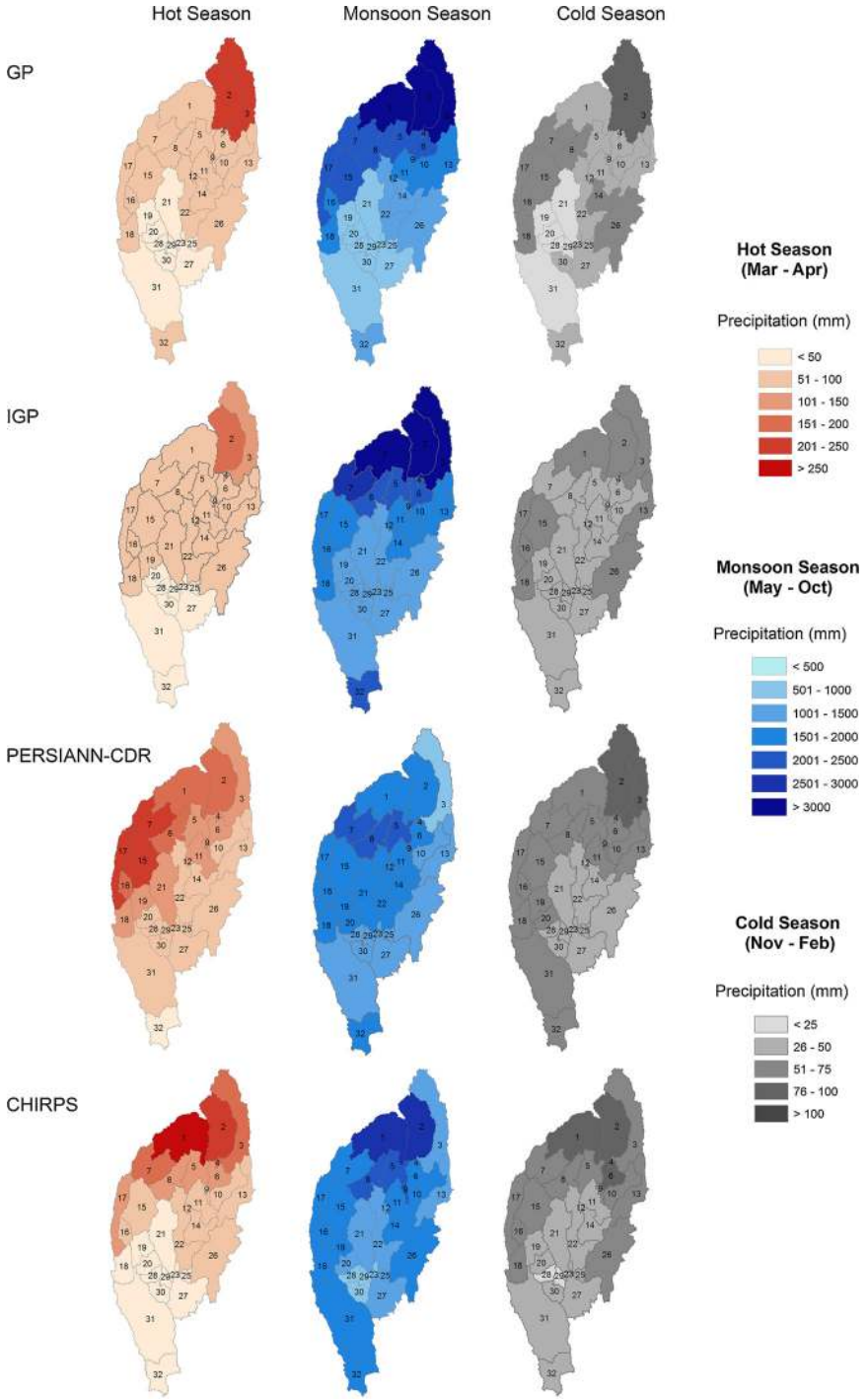

Fig. 4. Spatial distribution of seasonal variations of four precipitation datasets for the period of 2001–2010.

variations of the four precipitation products are different for each season. The most upstream parts of the basin (sub-basins 1, 2, and 3) receive higher precipitation than other sub-basins during all seasons. During the hot season, GP, IGP, and CHIRPS precipitation values decrease towards the southern parts of the basin, while PERSIANN-CDR data shows higher precipitation in the north-western and western parts of the basin. During the monsoon season, all the sub-basins receive more than 700 mm of precipitation in all the datasets used. During the same period, sub-basins 1, 2, and 3 receive more than 3500 mm precipitation, which is also the highest for the entire Irrawaddy Basin. These computed precipitations of the basins mainly rely on Hkamti (Sub-basin 1) and Putao (Sub-basins 2 and 3) stations. Compared to IGP data, PERSIANN-CDR and CHIRPS data show less precipitation within the north-eastern and north-

Fig. 5. Comparison of simulated and observed monthly stream flow of best simulation at a) Monywa b) Sagaing and c) Pyay during Calibration (1991–2000) and Validation (2002–2010) periods.

western parts of the basin. During the cold season, spatial variations in the total precipitation resulting from the IGP dataset are the least in all the sub-basins considered. The highest variability can be observed in CHIRPS precipitation over the basin. In terms of basin-wide seasonal precipitation, the highest precipitations during the hot (120 mm), monsoon (1927 mm), and cold (60 mm) seasons are observed in PERSIANN-CDR, IGP, and CHIRPS, respectively. Similarly, the lowest precipitation during the same seasons can be observed from IGP (70 mm), PERSIANN-CDR (1635 mm), and GP (49 mm), respectively.

PERSIANN-CDR shows the lowest average annual rainfall over all the sub-basins. These results are consistent with findings of Miao et al. (2015). They found that compared to the ground-based East Asia (EA) precipitation product, PERSIANN-CDR slightly underestimated the extreme rainfall events over China. Global products (PERSIANN-CDR and CHIRPS) produce less rainfall amount compared to observed data, particularly in the high altitude regions of the basin. Le and Pricope (2017) also showed that the CHIRPS dataset provides less accurate results for high altitude regions of the Nzoia Basin in Kenya. However, other studies on CHIRPS, which are also based in complex topographic regions (Funk et al., 2015; Katsanos et al., 2016; Shrestha et al., 2017) do not mention any lapses in the model performances. In general, the four datasets show considerably varied precipitation across the basin (Fig. 3 and Fig. 4). Given that precipitation is considered to be the primary forcing data for hydrological model simulation, such differences in precipitation inputs are expected to cause variations in the outcomes of the hydrological simulations.

3.2. Evaluation of simulated streamflows

The comparison of the observed and model simulated streamflows indicates that models based on observed precipitation (GP and IGP) outperform those based on global data sources (PERSIANN-CDR and CHIRPS) in both calibration (1991–2000) and validation (2002–2010) (Fig. 5, Table 4 and Supplementary information S1). Models that utilize GP data slightly overestimate extreme events, whereas simulations with PERSIANN-CDR and CHIRPS perform relatively poorly during the high flow periods. Particularly, for the year 2002, high flows were overestimated at the Katha, Sagaing, Monywa and Nyuang U stations. Simulated streamflow with the GP dataset at the Hkamti and Homalin stations showed better agreement with observed streamflow than with the other precipitation

Table 4
SWAT model performance for calibration and validation periods.

Period	Station	NSE				R2				PBIAS			
		GP	IGP	PERSIANN-CDR	CHIRPS	GP	IGP	PERSIANN-CDR	CHIRPS	GP	IGP	PERSIANN-CDR	CHIRPS
Calibration (1991–2000)	Hkamti	**0.93**	0.86	0.59	0.73	**0.93**	0.92	0.83	0.86	**−0.6**	−22.6	−40.5	−26.1
	Homalin	**0.92**	0.91	0.70	0.78	**0.93**	**0.93**	0.84	0.87	**−3.5**	−10.7	−29.0	−21.7
	Kalewa	0.94	**0.95**	0.85	0.86	0.94	**0.96**	0.89	0.92	**−4.1**	−5.5	−13.6	−15.4
	Monywa	0.92	**0.95**	0.89	0.91	0.93	**0.95**	0.89	0.93	**0.7**	1.6	1.8	−8.8
	Katha	0.69	**0.91**	0.35	0.75	0.86	**0.92**	0.80	0.89	5.8	**−4.9**	−48.5	−29.1
	Sagaing	0.82	**0.83**	0.28	0.58	0.85	**0.90**	0.80	0.86	**−11.1**	−19.7	−49.8	−38.2
	Nyaung U	0.90	**0.93**	0.87	0.92	**0.95**	**0.95**	0.90	0.94	5.8	**2.3**	−11.2	−10.5
	Pyay	**0.94**	0.93	0.86	0.91	**0.94**	**0.94**	0.88	0.92	**−0.1**	4.3	−7.4	−7.7
Validation (2002–2010)	Hkamti	0.85	**0.93**	0.55	0.74	0.93	**0.94**	0.78	0.79	20.9	**−10.7**	−42.5	−17.9
	Homalin	0.91	**0.94**	0.61	0.76	0.94	**0.95**	0.83	0.77	1.1	−10.6	−37.9	**8.2**
	Kalewa	0.90	**0.97**	0.85	0.87	0.95	**0.97**	0.91	0.92	8.9	**−1.5**	−16.2	−11.9
	Monywa	0.75	**0.95**	0.93	0.91	0.95	**0.97**	0.93	0.91	27.9	8.6	**0.7**	4.8
	Katha	0.56	**0.90**	0.12	0.76	0.84	**0.92**	0.68	0.88	9.3	**−2.4**	−50.1	−23.7
	Sagaing	0.81	**0.89**	0.42	0.72	0.85	**0.90**	0.80	0.89	**−1.1**	−9.1	−44.2	−30
	Nyaung U	0.81	0.91	0.92	**0.95**	0.94	**0.96**	0.93	0.95	22.7	8.3	−3.9	**2.0**
	Pyay	0.91	**0.96**	0.89	0.93	0.95	**0.96**	0.91	0.93	13.5	4.9	−4.1	**1.7**

Note: The highest values of each performance indicator are highlighted in Bold.

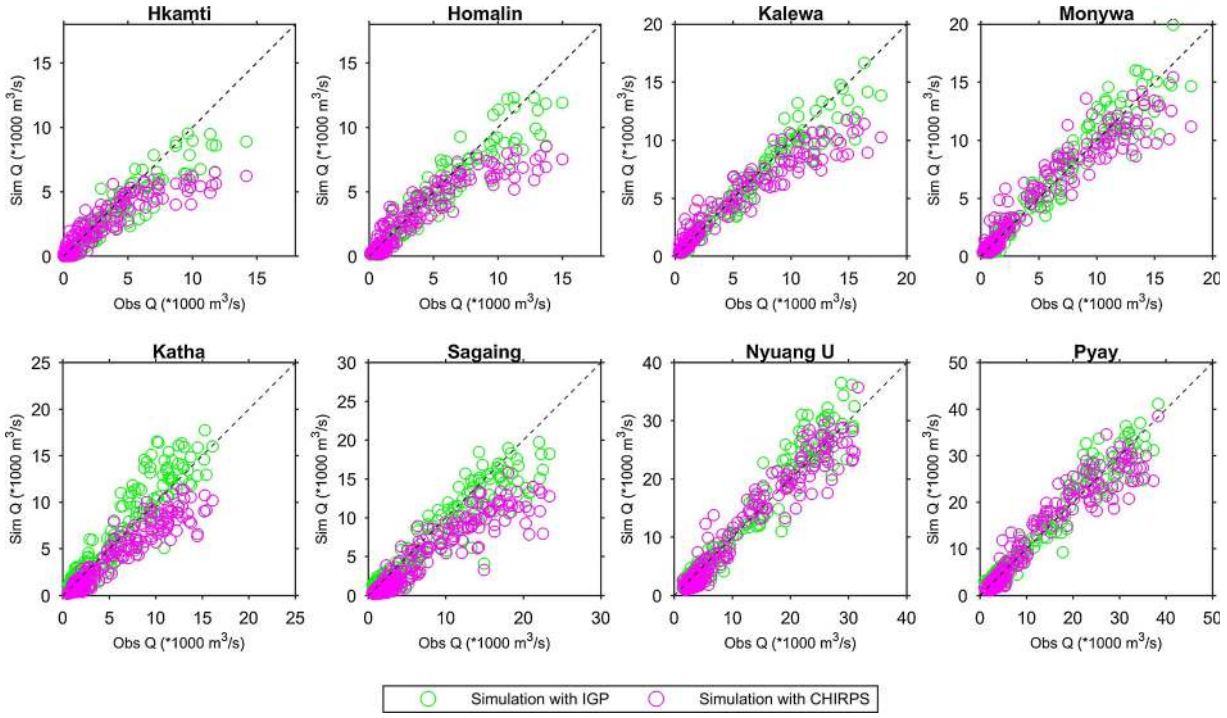

Fig. 6. Comparison of simulated monthly streamflow (forced with IGP and CHIRPS) and observed monthly streamflow at the gauging stations.

datasets. These two stations represent Sub-basins 1 and 7, respectively, each containing a rainfall gauging station. During the low flow period, simulations with all four datasets showed similar levels of accuracies. However, at the Katha and Sagaing stations, simulated streamflows with PERSIANN-CDR and CHIRPS were lower than the observed flow values. Models forced with CHIRPS inputs adequately reproduced the observed streamflow at Homalin, Kalewa, Monywa, Nyaung U, and Pyay.

Table 4 presents the statistical performance indicators (NSE, R^2, and PBIAS) of the hydrological simulations (streamflow) at eight gauging locations for the calibration and validation periods. The highest NSE and R^2 and lowest PBIAS among the four cases have been highlighted. For the calibration, R^2 varied within 0.8 to 0.96, while the NSE and PBIAS varied from 0.28 to 0.95 and −49.8% to 5.8%, respectively. All the models produced better results at Hkamti, Homalin, Kalewa, and Monywa gauging stations in the Chindwin River Basin than at the Katha and Sagaing stations located in the upper Irrawaddy Basin.

According to the model evaluation criteria proposed by Moriasi et al. (2007) (see Section 2.3), performances of the models driven by GP and IGP were 'very good' in both calibration and validation at all stations, except the simulation with GP data at the Katha station that showed only 'good' performance. PERSIANN-CDR driven simulations showed varied performances at different stations. For example, the lowest NSE (0.28) and the highest PBIAS (-49.8%) were obtained at the Sagaing station, while the highest NSE (0.89) and the lowest PBIAS (1.8%) were observed at the Monywa station. Similarly, simulations with CHIRPS showed 'satisfactory' results at the Sagaing and Hkamti stations, whereas the model performances at the other stations were 'very good' in both calibration and validation.

Fig. 6 compares the observed monthly streamflow versus the streamflow simulations forced by IGP and CHIRPS at eight gauging stations. Correlation coefficient values (R^2) for the simulations forced with IGP and CHIRPS are more than 0.84 and 0.81, respectively. Simulations with IGP have showed a good agreement with observed data with the exception of overestimated streamflow values at the Katha station. In contrast, models forced with CHIRPS tended to underestimate the streamflow at the Hkamti, Katha, and Sagaing stations. These relatively low values for streamflow simulation forced by CHIRPS can be attributed to the under-estimation of precipitation by CHIRPS in the high altitude regions of the basin.

PERSIANN-CDR had the lowest total precipitation compared to the other datasets; thus, the simulations driven with PERSIANN-CDR data tended to underestimate high streamflows and demonstrate weaker model performance in terms of NSE and PBIAS. During the monsoon season, both PERSIANN-CDR and CHIRPS yielded less precipitation over the eastern and northern parts of the basin, thus simulations with those datasets significantly underestimate the high flows at Hkamti, Katha and Sagaing stations than at the other stations. During the hot and cold seasons, all the models showed reasonable agreements with the observed streamflow. However, R^2 values were greater than 0.8 at all the gauging stations for both the calibration and validation periods. Despite overestimating the high flows at all the gauging stations, simulations forced with the GP dataset satisfactorily reproduced the observed flow in the entire study area. Although the average rain gauge density of Irrawaddy Basin is approximately 20,000 km^2 per station, which is very low compared to the minimum requirement stated in the WMO guidelines (5,750 km^2 per station for interior plains), the models driven by IGP managed to reproduce the measured streamflow at all the stations. This indicates that the interpolation of

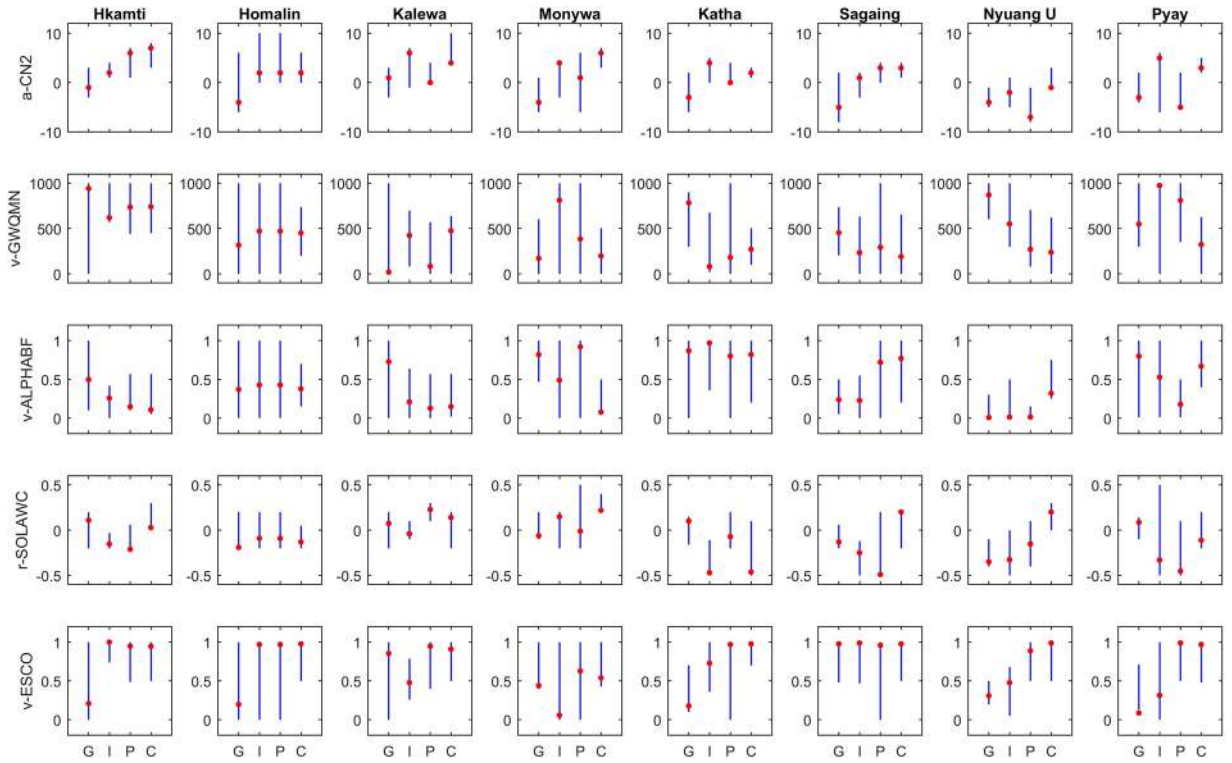

Fig. 7. Five selected global parameters with their initial range indicated by the blue line and fitted values in red dots for the four models with different precipitation inputs, v- denotes to replace the existing value; a- denotes to add a fixed value to the existing value and r- denotes to the relative change of the existing value. G- Gauge precipitation, I- Interpolated gauge precipitation, P- PERSIANN-CDR, and C-CHIRPS. Note: Corresponding parameter changes in sub-basins for each stations: Hkamti - 1, Homalin - 6 and 7, Kalewa- 15, Monywa - 16,17,18,19 and 20, Katha - 2,3,4,5,6,9,10 and 11, Sagaing - 12, 13, 14 and 22, Nyaung U - 21,23,24,25,26,27,28,29 and 30 and Pyay - 31,32.

gauge data may lead to an improved representation of precipitation over the basin. In most cases, PERSIANN-CDR and CHIRPS also showed good agreement with observed streamflow in terms of NSE and R^2, however, their biases were higher than the biases of simulations forced with IGP. In general, CHIRPS driven simulations performed better than simulations forced with PERSIANN-CDR. Therefore, the CHIRPS product can be utilized as an alternative source of rainfall inputs for hydrological studies in the Irrawaddy Basin. Tuo et al. (2016) have also suggested CHIRPS data as a favorable choice for data scarce Alpine regions. Apart from that, Le and Pricope (2017) concluded that the use of CHIRPS data with the SWAT model significantly improved the streamflow volume estimation, but not the satisfactory efficiency criteria, for the Nzoia Basin, Kenya. Further, as discussed by Faridzad et al. (2018), despite having limitations and uncertainties, the bias-corrected PERSIANN-CDR data provides valuable information for hydrological simulation in remote and high altitude areas.

3.3. Uncertainty in runoff simulation

During the model calibration, 14 selected hydrological parameters were adjusted and converged to different optimal intervals to reproduce streamflows at eight gauging stations. While noting that sensitivities of the parameters can be basin specific, five globally sensitive hydrological parameters have been selected to discuss these results (Fig. 7). Curve Number (CN2) corresponds to the land use type and largely affects surface runoff generation. The four precipitation inputs used in this study led to different best fit CN2 values (a_CN2 varies −7 to 7) and ranges. For the simulations with GP, fitted parameter values significantly deviated from those obtained through simulations with the other three precipitation inputs. Hence, a common pattern for fitted parameters could not be identified for all sub-basins. GW_QMN is an important parameter, related to base flow. During low flow periods, groundwater contribution to streamflow can be significant. There is an apparent variability in these fitted parameters for most of the sub-basins, where the highest variability for this parameter (v_GWQMN from 81 to 874) was observed in the sub-basins corresponding to the Katha station. Compared to CN2, the variability of the fitted GW_QMN for the four models at each sub-basin was high. The base flow recession factor (ALPHA_BF) can vary between 0 and 1. The sub-basins corresponding to the Hkamti, Homalin and Nyaung U stations resulted in nearly equal best fit ALPHA_BF for all precipitation datasets. SOL_AWC is related to the available water content in the soil. The best-fitted parameters (i.e. relative changes of existing value of SOL_AWC) varied from −0.49 to 0.23. Fitted parameter values for ESCO, which is relevant for soil evaporation, varies between default SWAT limits (0–1) for the precipitation inputs considered. All the fitted parameters are tabulated in Supplementary information S1.

Table 5
Prediction uncertainty in simulated streamflow.

Period	Station	P-factor				r-factor			
		GP	IGP	PERSIANN -CDR	CHIRPS	GP	IGP	PERSIANN -CDR	CHIRPS
Calibration (1991–2000)	Hkmathi	0.75	0.77	0.46	0.56	0.30	0.39	0.21	0.23
	Homalin	0.65	0.58	0.48	0.25	0.40	0.40	0.32	0.19
	Kalewa	0.72	0.85	0.78	0.69	0.40	0.45	0.53	0.28
	Monywa	0.48	0.86	0.79	0.57	0.11	0.61	0.62	0.26
	Katha	0.88	0.63	0.38	0.32	0.96	0.34	0.54	0.27
	Sagaing	0.43	0.61	0.20	0.13	0.31	0.51	0.31	0.11
	Nyaung U	0.70	0.76	0.73	0.36	0.48	0.64	0.63	0.16
	Pyay	0.52	0.53	0.50	0.33	0.25	0.37	0.33	0.16
Validation (2001–2010)	Hkmathi	0.56	0.82	0.43	0.45	0.23	0.44	0.23	0.26
	Homalin	0.63	0.56	0.08	0.40	0.46	0.45	0.10	0.12
	Kalewa	0.84	0.93	0.75	0.69	0.51	0.51	0.54	0.31
	Monywa	0.33	0.87	0.83	0.56	0.12	0.69	0.66	0.30
	Katha	0.88	0.63	0.25	0.24	0.85	0.37	0.51	0.29
	Sagaing	0.47	0.64	0.35	0.24	0.33	0.55	0.30	0.11
	Nyaung U	0.62	0.78	0.82	0.66	0.49	0.62	0.59	0.16
	Pyay	0.46	0.58	0.43	0.48	0.29	0.36	0.31	0.07

Prediction uncertainties (P-factor and r-factor) of streamflow simulations are presented for the four precipitation products (Table 5). In calibration, IGP data driven simulations captured more than 53% of the observations at all the stations within the 95PPU band and together with a r-factor (average band width) from 0.34 to 0.69. IGP driven simulations also showed more consistent prediction uncertainties for both calibration and validation periods than did the other three precipitation products. Simulations with PERSIANN-CDR and CHIRPS showed the considerably higher variability of P-factors compared to those with GP and IGP. For example, in calibration, the P-factor variations are 0.2 to 0.79 for PERSIANN-CDR and 0.13 to 0.69 for CHIRPS. Overall, the average P-factors among the eight gauging stations are pretty low: 0.62, 0.71, 0.52, and 0.43 for GP, IGP, PERSIANN-CDR, and CHIRPS, respectively. This shows that the uncertainty measures estimated based on parameter uncertainty (parameter ranges) were unable to capture all sources of uncertainty. It implies that a considerable amount of uncertainty cannot be attributed to parameter uncertainty, and comes notably from precipitation.

4. Conclusion

This study investigated the dependency between different precipitation data sources and the reliability of the resulting modelled streamflows for the Irrawaddy Basin in Myanmar. Four precipitation data sets used are in-situ gauge data without interpolation and with interpolation, PERSIANN-CDR, and CHIRPS. We analyzed the spatial and temporal distribution of the four precipitation datasets and their impacts on streamflow simulation in the Irrawaddy Basin.

The four precipitation datasets are different in magnitude and spatial and temporal distributions over the study area. The global data sources (PERSIANN-CDR and CHIRPS) yielded lower annual and seasonal precipitation compared to the in-situ gauge data. Interpolated gauge data showed the highest basin average precipitation during the monsoon season (May-Oct), whereas PERSIANN-CDR and CHIRPS showed the highest precipitations during the hot season (Mar-Apr) and cold season (Nov-Feb), respectively. Contradictory results were observed in the mountainous regions of the Irrawaddy Basin, where PERSIANN-CDR and CHIRPS data deviated notably from the interpolated gauge data.

During the monsoon period, simulations with observed data showed an overestimation of streamflow, while models with global products (PERSIANN-CDR and CHIRPS) tended to underestimate the same. Compared to the minimum rain gauge density guidelines provided by WMO (5750 km^2 per station for interior plains), the rain gauge density over the study area is very low (20,000 km^2 per station on an average). Despite the low density of rain gauges, in general, simulations with interpolated gauge precipitation data showed a good agreement with observed streamflow data for all the stations in the basin. A majority of the stations also showed good results in simulations forced with CHIRPS and PERSIANN-CDR in terms of NSE and R^2, however with higher biases. It is to be noted that the in-situ gauge data used here is available only for 20 years. Because the CHIRPS and PERSIANN-CDR products have longer periods of records (more than 35 years), they can be valuable assets for data poor river basins for hydrological applications requiring long data records. Another potential application of these global data is to develop a merged product combining gauged data and one or more global data products. Different precipitation inputs lead to different best fitted parameter values and ranges for the different sub catchments. Overall, we found that different precipitation datasets have considerable impacts on a model performance, parameter estimation and uncertainty in streamflow simulations.

Declarations of interest

None.

Acknowledgments

JGS is supported by the Netherlands Fellowship Programme (NFP). RR is supported by the AXA Research Fund and the Deltares Harbour, Coastal and Offshore Research Program. The model simulations were carried out on the Dutch national e-infrastructure with the support of SURF Cooperative.

Appendix A. Supplementary data

Supplementary material related to this article can be found, in the online version, at doi:https://doi.org/10.1016/j.ejrh.2018.10.005.

References

Abbaspour, K.C., 2015. SWAT-Calibration and Uncertainty Programs (CUP). https://doi.org/10.1007/s00402-009-1032-4.
Abbaspour, K.C., Johnson, C.A., van Genuchten, M.T., 2004. Estimating uncertain flow and transport parameters using a sequential uncertainty fitting procedure. Vadose Zone J. 3, 1340–1352. https://doi.org/10.2136/vzj2004.1340.
Abbaspour, K.C., Rouholahnejad, E., Vaghefi, S., Srinivasan, R., Yang, H., Kløve, B., 2015. A continental-scale hydrology and water quality model for Europe: calibration and uncertainty of a high-resolution large-scale SWAT model. J. Hydrol. (Amst) 524, 733–752. https://doi.org/10.1016/j.jhydrol.2015.03.027.
Abbaspour, K.C., Yang, J., Maximov, I., Siber, R., Bogner, K., Mieleitner, J., Zobrist, J., Srinivasan, R., 2007. Modelling hydrology and water quality in the pre-alpine/alpine Thur watershed using SWAT. J. Hydrol. (Amst) 333, 413–430. https://doi.org/10.1016/j.jhydrol.2006.09.014.
Andreassian, V., Perrin, C., Michel, C., Sanchez, I.U., Lavabre, J., 2001. Impact of imperfect rainfall knowledge on the effciency and the parameters of watershed models. J. Hydrol. (Amst) 250, 206–223.
Arnold, J.G., Srinivasan, R., Muttiah, R.S., Williams, J.R., 1998. Large area hydrologic modeling and assesment part I: model development. JAWRA J. Am. Water Resour. Assoc. 34, 73–89. https://doi.org/10.1111/j.1752-1688.1998.tb05961.x.
Ashouri, H., Hsu, K.L., Sorooshian, S., Braithwaite, D.K., Knapp, K.R., Cecil, L.D., Nelson, B.R., Prat, O.P., 2015. PERSIANN-CDR: daily precipitation climate data record from multisatellite observations for hydrological and climate studies. Bull. Am. Meteorol. Soc. 96, 69–83. https://doi.org/10.1175/BAMS-D-13-00068.1.
Ashouri, H., Nguyen, P., Thorstensen, A., Hsu, K.-L., Sorooshian, S., Braithwaite, D., 2016. Assessing the efficacy of high-resolution satellite-based PERSIANN-CDR precipitation product in simulating streamflow. J. Hydrometeorol 17, 2061–2076. https://doi.org/10.1175/JHM-D-15-0192.1.
Bárdossy, A., Das, T., 2006. Influence of rainfall observation network on model calibration and application. Hydrol. Earth Syst. Sci. Discuss. 3, 3691–3726. https://doi.org/10.5194/hessd-3-3691-2006.
Beck, H.E., Vergopolan, N., Pan, M., Levizzani, V., van Dijk, A.I.J.M., Weedon, G., Brocca, L., Pappenberger, F., Huffman, G.J., Wood, E.F., 2017. Global-scale evaluation of 22 precipitation datasets using gauge observations and hydrological modeling. Hydrol. Earth Syst. Sci. Discuss. 21, 1–23. https://doi.org/10.5194/hess-2017-508.
Casse, C., Gosset, M., 2015. Analysis of hydrological changes and flood increase in Niamey based on the PERSIANN-CDR satellite rainfall estimate and hydrological simulations over the 1983–2013 period. IAHS-AISH Proc 370, 117–123. https://doi.org/10.5194/piahs-370-117-2015. Reports.
Ceccherini, G., Ameztoy, I., Hernandez, C.P.R., Moreno, C.C., 2015. High-resolution precipitation datasets in South America and West Africa based on satellite-derived rainfall, enhanced vegetation index and digital elevation model. Remote Sens. (Basel) 7, 6454–6488. https://doi.org/10.3390/rs70506454.
FAO, 2003. The Digital Soil Map of the World (Version 3.6). FAO/UNESCO, Rome, Italy.
Faridzad, M., Yang, T., Hsu, K., Sorooshian, S., Xiao, C., 2018. Rainfall frequency analysis for ungauged regions using remotely sensed precipitation information. J. Hydrol. (Amst) 563, 123–142. https://doi.org/10.1016/j.jhydrol.2018.05.071.
Funk, C., Peterson, P., Landsfeld, M., Pedreros, D., Verdin, J., Shukla, S., Husak, G., Rowland, J., Harrison, L., Hoell, A., Michaelsen, J., 2015. The climate hazards infrared precipitation with stations - a new environmental record for monitoring extremes. Sci. Data 2https://doi.org/10.1038/sdata.2015.66. 150066.
Guo, H., Chen, S., Bao, A., Hu, J., Gebregiorgis, A.S., Xue, X., Zhang, X., 2015. Inter-comparison of high-resolution satellite precipitation products over Central Asia. Remote Sens. (Basel) 7, 7181–7211. https://doi.org/10.3390/rs70607181.
Hassels, T., 2015. Comparison and Validation of Several Open Access Remotely Sensed Rainfall Products for the Nile Basin. Technical University of Delft, The Netherlands.
Her, Y., Frankenberger, J., Chaubey, I., Srinivasan, R., 2015. Threshold effects in HRU definition of the soil and water assessment tool. Am. Soc. Agric. Biol. Eng. 58, 367–378. https://doi.org/10.13031/trans.58.10805.
Jarvis, A., Reuter, H.I., Nelson, A., Guevara, E., 2008. Hole-filled SRTM for the Globe Version 4. available from the CGIAR-CSI SRTM 90m Database [WWW Document]. http://srtm.csi.cgiar.org).
Katsanos, D., Retalis, A., Michaelides, S., 2016. Validation of a high-resolution precipitation database (CHIRPS) over Cyprus for a 30-year period. Atmos. Res. 169, 459–464. https://doi.org/10.1016/j.atmosres.2015.05.015.
Le, A.M., Pricope, N., 2017. Increasing the accuracy of runoff and streamflow simulation in the Nzoia Basin,Western Kenya, through the incorporation of satellite-rerived CHIRPS Data. Water 9, 1–15. https://doi.org/10.3390/w9020114.
Legates, D.R., McCabe Jr, G.J., 1999. Evaluating the use of “Goodness of Fit” measures in hydrologic and hydroclimatic model validation. Water Resour. Res. 35, 233–241. https://doi.org/10.1029/1998WR900018.
Liu, X., Yang, T., Hsu, K., Liu, C., Sorooshian, S., 2017. Evaluating the streamflow simulation capability of PERSIANN-CDR daily rainfall products in two river basins on the Tibetan Plateau. Hydrol. Earth Syst. Sci. Discuss. 21, 169–181. https://doi.org/10.5194/hess-21-169-2017.
Lopez, M.G., Wennerstorm, H., Norden, L.-A., Seibert, J., 2015. Location and density of rain gauges for the Estimation of Spatial varying precipitation. Bull. Geogr. Phys. Geogr. Ser. 97, 167–179. https://doi.org/10.1111/geoa.12094.
Masih, I., Maskey, S., Uhlenbrook, S., Smakhtin, V., 2011. Assessing the impact of areal precipitation input on streamflow simultions usimg the SWAT model. J. Am. Water Resour. Assoc. 47, 179–195. https://doi.org/10.1111/j.1752-1688.2010.00502.x.
Maskey, S., 2013. HyKit: A Tool for Grid-based Interpolation of Hydrological Variables, User’s Guide (Version 1.3).
Massari, C., Crow, W., Brocca, L., 2017. An assessment of the accuracy of global rainfall estimates without ground-based observations. Hydrol. Earth Syst. Sci. Discuss. 21, 4347–4361. https://doi.org/10.5194/hess-2017-163.
Miao, C., Ashouri, H., Hsu, K.-L., Sorooshian, S., Duan, Q., 2015. Evaluation of the PERSIANN-CDR daily rainfall estimates in capturing the behavior of extreme precipitation events over China. J. Hydrometeorol. 16, 1387–1396. https://doi.org/10.1175/JHM-D-14-0174.1.
Moon, J., Srinivasan, R., Jacobs, J.H., 2004. Stream flow estimation using spatially distributed rainfall in the Trinity River Basin, Texas. Trans. ASAE 47, 1445–1452. https://doi.org/10.13031/2013.17624.
Moriasi, D.N., Arnold, J.G., Van Liew, M.W., Binger, R.L., Harmel, R.D., Veith, T.L., 2007. Model evaluation guidelines for systematic quantification of accuracy in watershed simulations. Am. Soc. Agric. Biol. Eng. 50, 885–900. https://doi.org/10.13031/2013.23153.
Moulin, L., Gaume, E., Obled, C., 2008. Uncertainties on mean areal precipitation: assessment and impact on streamflow simulations. Hydrol. Earth Syst. Sci. Discuss. 5, 2067–2110. https://doi.org/10.5194/hessd-5-2067-2008.
Neitsch, S.L., Arnold, J.G., Kiniry, J.R., Williams, J.R., 2011. Soil & Water Assessment Tool Theoretical Documentation Version 2009. Texas Water Resources Institute, TR-406, Texas. https://doi.org/10.1016/j.scitotenv.2015.11.063.

Pechlivanidis, I.G., Jackson, B.M., Mcintyre, N.R., Wheater, H.S., 2011. Catchment scale hydrological modelling: a review of model types, calibration approaches and uncertainty analysis methods in the context of recent developments in technology and applications. Glob. NEST 13, 193–214.
Price, K., Purucker, S.T., Kraemer, S.R., Babendreier, J.E., Knightes, C.D., 2014. Comparison of radar and gauge precipitation data in watershed models across varying spatial and temporal scales. Hydrol. Process. 28, 3505–3520. https://doi.org/10.1002/hyp.9890.
Pushpalatha, R., Perrin, C., Moine, N., Le, Andréassian, V., 2012. A review of efficiency criteria suitable for evaluating low-flow simulations. J. Hydrol. (Amst) 420–421, 171–182. https://doi.org/10.1016/j.jhydrol.2011.11.055.
Qian, W., Lee, D.-K., 2000. Seasonal march of the East-Asian summer monsoon. Int. J. Climatol. 20, 1371–1386.
Quenouille, A.M.H., 1956. Notes on bias in estimation. Biometrika 43, 353–360. https://doi.org/10.2307/2332914.
Segond, M., Wheater, H.S., Onof, C., 2007. The significance of spatial rainfall representation for flood runoff estimation: a numerical evaluation based on the Lee catchment, UK. J. Hydrol. 347, 116–131. https://doi.org/10.1016/j.jhydrol.2007.09.040.
Seibert, J., Vis, M.J.P., 2012. Teaching hydrological modeling with a user-friendly catchment-runoff-model software package. Hydrol. Earth Syst. Sci. Discuss. 16, 3315–3325. https://doi.org/10.5194/hess-16-3315-2012.
Shrestha, B., Babel, M.S., Maskey, S., Van Griensven, A., Uhlenbrook, S., Green, A., Akkharath, I., 2013. Impact of climate change on sediment yield in the Mekong River basin: a case study of the Nam Ou basin, Lao PDR. Hydrol. Earth Syst. Sci. 17, 1–20. https://doi.org/10.5194/hess-17-1-2013.
Shrestha, N.K., Qamer, F.M., Pedreros, D., Murthy, M.S.R., Wahid, S.M., Shrestha, M., 2017. Evaluating the accuracy of Climate Hazard Group (CHG) satellite rainfall estimates for precipitation based drought monitoring in Koshi basin, Nepal. J. Hydrol. Reg. Stud. 13, 138–151. https://doi.org/10.1016/j.ejrh.2017.08.004.
Tan, M.L., Gassman, P.W., Cracknell, A.P., 2017. Assessment of three long-term gridded climate products for hydro-climatic simulations in tropical river basins. Water 9, 1–24. https://doi.org/10.3390/w9030229.
Thiemig, V., Rojas, R., Zambrano-Bigiarini, M., De Roo, A., 2013. Hydrological evaluation of satellite-based rainfall estimates over the Volta and Baro-Akobo Basin. J. Hydrol. (Amst) 499, 324–338. https://doi.org/10.1016/j.jhydrol.2013.07.012.
Toté, C., Patricio, D., Boogaard, H., van der Wijngaart, R., Tarnavsky, E., Funk, C., 2015. Evaluation of satellite rainfall estimates for drought and flood monitoring in Mozambique. Remote Sens. (Basel) 7, 1758–1776. https://doi.org/10.3390/rs70201758.
Tuo, Y., Duan, Z., Disse, M., Chiogna, G., 2016. Evaluation of precipitation input for SWAT modeling in Alpine catchment: a case study in the Adige river basin (Italy). Sci. Total Environ. 573, 66–82. https://doi.org/10.1016/j.scitotenv.2016.08.034.
Vu, M.T., Raghavan, S.V., Liong, S.Y., 2012. SWAT use of gridded observations for simulating runoff - a Vietnam river basin study. Hydrol. Earth Syst. Sci. Discuss. 16, 2801–2811. https://doi.org/10.5194/hess-16-2801-2012.
Yatagai, A., Kamiguchi, K., Arakawa, O., Hamada, A., Yasutomi, N., Kitoh, A., 2012. Aphrodite constructing a long-term daily gridded precipitation dataset for Asia based on a dense network of rain gauges. Bull. Am. Meteorol. Soc. 93, 1401–1415. https://doi.org/10.1175/BAMS-D-11-00122.1.
Zhu, Q., Hsu, K., Xu, Y.-P., Yang, T., 2017. Evaluation of a new satellite-based precipitation data set for climate studies in the Xiang River basin, southern China. Int. J. Climatol. 37, 4561–4575. https://doi.org/10.1002/joc.5105.